Review

Suresh Thareja, Mengyuan Zhu, Xingyue Ji* and Binghe Wang*

Boron-based small molecules in disease detection and treatment (2013–2016)

DOI 10.1515/hc-2017-0086
Received April 27, 2017; accepted May 8, 2017; previously published online June 14, 2017

Abstract: Recent years have seen tremendous development in the design and synthesis of boron-based compounds as potential therapeutics and for detection applications. The present review highlights the most recent development of these boron-based small molecules, covering clinically used ixazomib, tavaborole, crisaborole and other molecules from 2013 to 2016.

Keywords: BNCT; boronic acid; cancer; carbohydrate; sensors; sugar.

Introduction

Boron is similar to carbon in size, can adopt both sp^2 and sp^3 forms and can mimic carbon in many ways. Yet, it is also unique in that in its neutral trivalent form, it has an open shell. Therefore, it serves as a good Lewis acid and is a 'hot' electrophile. An additional property of boron is its ability to emit alpha particles under neutron bombardment. This is also the basis for using boron-based molecules in boron neutron capture therapy (BNCT). All these properties are useful for boron's various applications. This review is divided into four sections: detection and sensing, disease treatment through binding to carbohydrates, disease treatment through binding to other biological targets and BNCT. There have been many good reviews, book chapters and books covering earlier work in these areas [1–11]. Therefore, this review will only cover the most recent developments from 2013 to 2016.

***Corresponding authors: Xingyue Ji and Binghe Wang,** Department of Chemistry and Center for Diagnostics and Therapeutics, Georgia State University, Atlanta, GA 30303, USA, e-mail: xji@gsu.edu (X. Ji); Wang@gsu.edu (B. Wang)
Suresh Thareja and Mengyuan Zhu: Department of Chemistry and Center for Diagnostics and Therapeutics, Georgia State University, Atlanta, GA, USA

Boronic acid-based sensors for disease detection

In disease detection, the utility of boron-based molecules is largely in carbohydrate recognition using the boronic acid (BA) moiety as a key recognition unit. There is a growing body of evidence demonstrating the very important roles of carbohydrates in physiological and pathological processes [12–14]. Often, carbohydrates serve as biomarkers for various pathological states and changes. This is especially true in cancer, as a significant percentage of cancer-associated antigens are carbohydrate-related [15]. Despite the importance of carbohydrates in disease, the field of BA-based chemosensors or binders for carbohydrate recognition disease detection is still in its infancy. There are several reasons that BA is a very useful functional group in this regard. First, it is a Lewis acid with a strong affinity for Lewis bases such as hydroxyl groups through the formation of covalent bonds. Second, the covalent bond formation is reversible in aqueous solution, which is very important because this reversibility in binding is critical to the detection of carbohydrates in a dynamic fashion in response to concentration changes. Third, many BAs have been designed in such a way that they would change spectroscopic properties in response to binding. This gives a reporting event for sensitive detection. Fourth, the BA group is polar and helps improve the water solubility of the chemosensor. This is important for sensing under near physiological conditions. Fifth, the parameters needed to tune the binding affinity of a BA group with a carbohydrate are well understood [16, 17]. This tremendously facilitates the development of BA-based chemosensors for carbohydrates.

BA-based fluorescence sensors

Commonly seen carbohydrates that are disease biomarkers include the Tn antigen, Globo-H, Lewis X (Le^x), Lewis Y (Le^y) and sialic acid (Sia) and its derivatives including sialyl Lewis X (sLe^x) and sialyl Lewis A (sLe^a). In the

following sections, we review recent developments of these types of sensors in disease detection.

Chu and co-workers developed a boronolectin-fluorophore conjugate **1** (Figure 1) to target sLe^x, a carbohydrate that is commonly overexpressed on the surface of cancer cells [18]. The design is based on an available sensor of sLe^x [19]. By introducing BODIPY D-10001, a long-wavelength fluorophore ($\lambda_{ex} = 651$ nm, $\lambda_{em} = 660$ nm), Chu made it feasible to detect subcutaneously implanted tumors *in vivo*. Specifically, compound **1** was injected (tail vein) into mice implanted with HEPG2 cells that express sLe^x and COLO2050 cells that express sLe^x and sLe^a. It was found that after a 24-h washout period, compound **1** selectively labeled the tumor. This was the first example of using boronolectin for selective recognition of xenograft tumors *in vivo*.

To make fluorescent sensors more water-soluble, Xu and co-workers prepared a series of peptide-based sensors (Figure 2). They tested compounds on four cancer-related glycans and found that compound **2a** could selectively recognize sLe^x *in situ*. It showed 7-fold selectivity for sLe^x over Le^x, 4-fold selectivity over Le^y and 3-fold selectivity over sLe^a [20]. The authors suggested that compound **2a** might also bind cancer-related integrin $\alpha_v\beta_3$ and $\alpha_v\beta_5$ because of its RGD sequence, making it a dual-targeting molecule.

Gao and co-authors synthesized compounds **3a** and **3b** (Figure 3) and found that compound **3a** can selectively

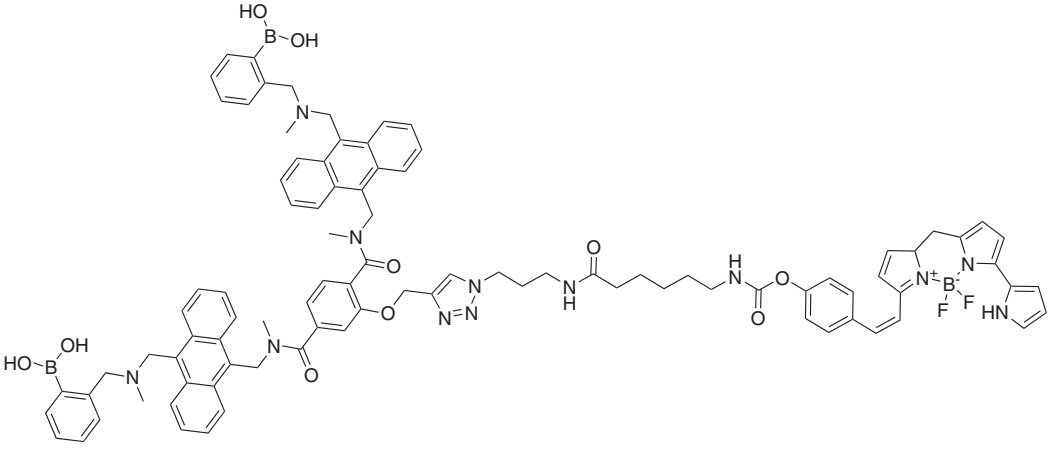

Figure 1 Boronolectin-fluorophore conjugate **1**.

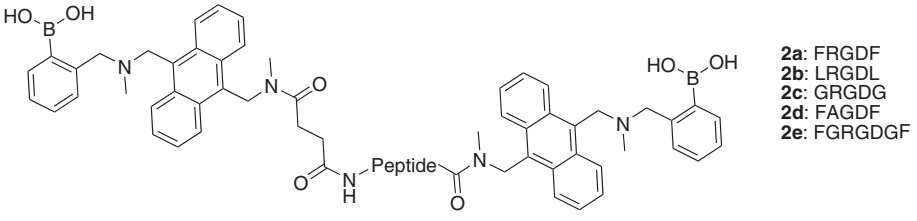

Figure 2 BA-based peptide sensors **2a–e** with the corresponding amino acid sequences.

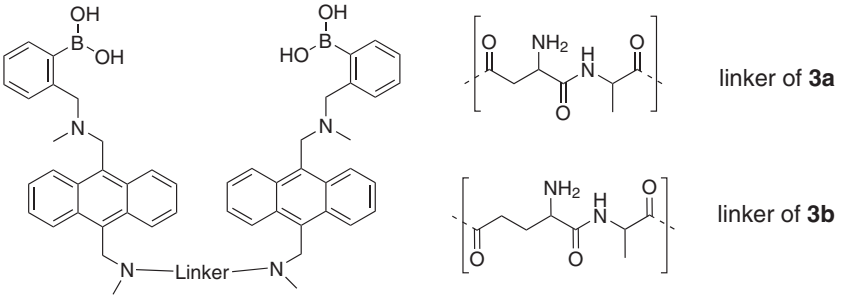

Figure 3 BA-based chemosensors **3a** and **3b**.

bind Le^x (CHOFUT4) over Le^y (HEP3B), sLe^a (B16FUT3 and COLO205) and sLe^x (COLO205) in cell labeling studies. This was the first synthetic chemosensor of Le^x [21].

To detect Sia on the cell surface, Chaudhary and co-workers developed peptidomimetic compounds **4a** and **4b** (Figure 4), on which the biotin moiety was used in conjugation with fluorescent streptavidin [22]. By treating compounds **4a** and **4b** with different concentrations of Sia, mannose, galactose and fructose, together with 0.05% Tween-20 and FITC-conjugated Cy3-streptavidin, the authors could detect fluorescence intensities. Through quantitative analysis of the results, they found that the dissociation constant for **4a** for Sia is 0.0754 μM while the values of the other three sugars are over 10 μM, indicating a good selectivity. Microarray and confocal imaging studies suggested that compound **4a**, similar to a commercial sialic acid-binding lectin-*Sambucus nigra* lectin (SNA), had interactions with Sia molecules on the cell surface. Their work provided a synthetic alternative to SNA.

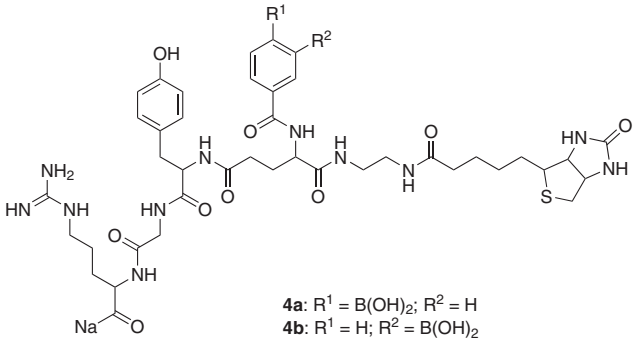

Figure 4 Structures of peptidomimetic BA compounds **4a** and **4b**.

Chang and co-workers reported three new fluorescent sensors (Figure 5) to recognize sLe^x. By testing their compounds with cell lines PLC/PRF/5 (sLe^x), HEPG2 (sLe^x), MDA-MB-231 (CD44), COLO205 (sLe^x and sLe^a) and COS7 (control), they noticed that compound **5b** could identify sLe^x. MTT studies showed that they were not toxic at 20 μM, and a Hoechst 33258 experiment showed that there was no apoptosis [23].

Other boronic acid-based reporters or sensors

To measure overexpressed glycoproteins in cells, Culf and co-workers synthesized boron-containing anthranilic acids (Figure 6) [24]. In MeOH solvent, compound **6** was found to possess the brightest fluorescence with a 64% quantum yield and a relatively large Stokes shift of 89 nm. Therefore, **6** was used in confocal microscopy fluorescence studies on normal cells (MCF10A) and cancer cells (MCF, MDA-MB-231, SKBR3, DLD-1, HCT116 and HT1080). It was found that all cancer cells, even less aggressive breast cancer cell lines (MCF7) and fibrosarcoma cell lines (HT1080), gave a blue emission upon exposure to **6**. However, **6** did not produce a blue emission with normal cells. The authors suggested that reporter **6** is selective to cancer cells because of their overexpressed glycoproteins.

Shinde and co-workers reported Sia-imprinted fluorescent core-shell polymeric particles for carbohydrate

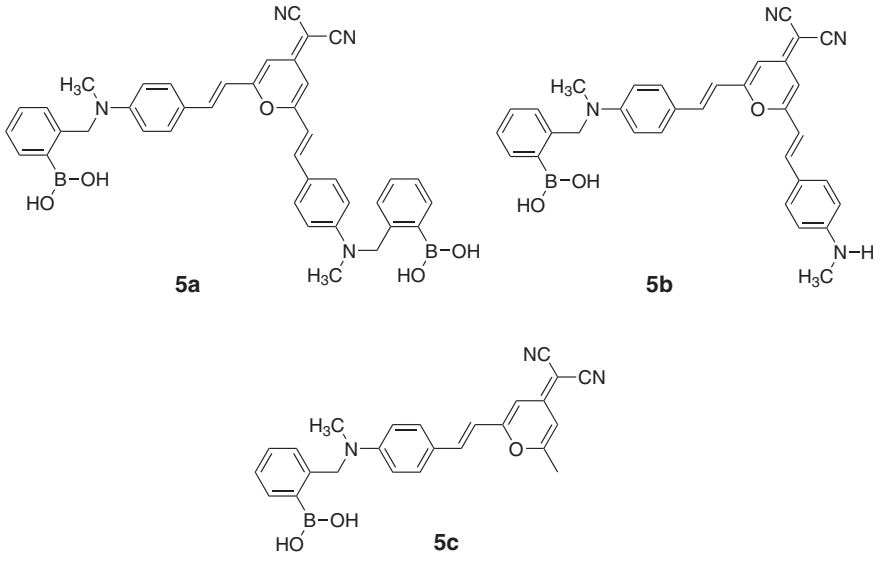

Figure 5 BA-based fluorescent sensors **5a**–**c**.

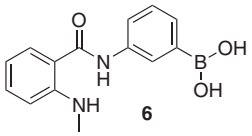

Figure 6 Boron-containing anthranilic acid sensor **6**.

detection [25]. Molecular imprinting is a process of building a polymeric cavity by polymerization in the presence of a template (the print molecule). In this case, the idea was to take advantage of (1) the reversible boronate ester formation between BA and Sia; (2) the ionic interactions between a cationic amino group and a carboxylate; and (3) the environmental sensitivity of the nitrobenzoxadiazole fluorophore to binding events. The monomers were grafted on silica core particles using ethylene glycol dimethacrylate (Figure 7) before polymerization. Their results showed that the imprinted particles are selective for Sia over glucuronic acid, with binding constants K of 5.9×10^{3} M^{-1} and 1.8×10^{3} M^{-1} for Sia and glucuronic acid, respectively. Cell staining using the imprinted polymer correlated with the Sia expression level.

Stephenson-Brown and co-workers also reported using imprinted polymers for glycoprotein recognition [26]. Thus, glycoprotein, BA and acrylamide were mixed together before the initiation of polymerization. The removal of the glycoprotein after polymerization leaves a well-shaped pocket, which is supposed to be complementary to the print glycoprotein. In this case, prostate-specific antigen (PSA) was used as the glycoprotein template. Surface plasmon resonance (SPR) analysis showed that the imprinted particles gave a 30-fold selectivity of PSA over horseradish peroxidase and at least a 2-fold selectivity over lysozyme, α-1-acid glycoprotein, RNAse B, bovine serum albumin and α-1-antitrypsin.

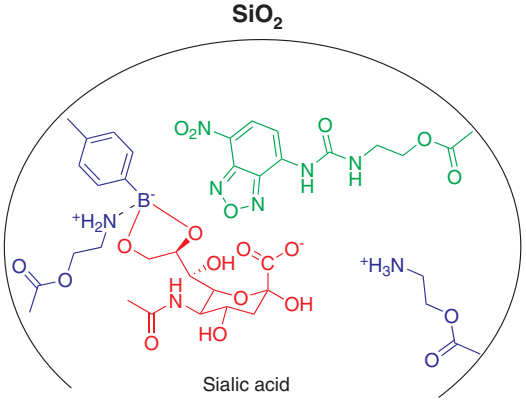

Figure 7 Sia-imprinted shell on silica core particles.

Zhang and co-workers used nanoparticles (NPs) to detect Sia using inductively coupled plasma mass spectrometry (ICP-MS) [27]. ICP-MS is a type of MS that can detect metals at concentrations as low as one part in 10^{15}. The design is based on the ability of biotinylated phenylboronic acid (biotin-APBA) **7** (Figure 8) to bind to Sia and the ability of gold NPs (AuNPs) to enhance the signal in ICP-MS. Specifically, the BA moiety of **7** was used for Sia recognition on tumor cell surfaces and streptavidin-conjugated AuNPs were tethered to **7** as elemental tags. Then, the system was incubated with cancer cell lines (MCF-7 and HepG2) for 1 h. After washing, the labeled AuNPs were released using acid and detected using ICP-MS. By adding different amounts of free Sia molecules to the sample, the authors could conduct competitive binding experiments to calculate the quantity of Sia on cell surfaces. With this method, the number of Sia molecules on the cell surface was identified as 7.0×10^{9} and 5.4×10^{9} for MCF-7 and HepG2 cell lines, respectively.

Therapeutics based on carbohydrate recognition

Compared to the detection of disease, the therapeutic potential of BA based on carbohydrate recognition is less developed and is primarily applied in two fields: BA-aided intracellular delivery of biomacromolecules and BA-functionalized polymer for the inhibition of virus infection. The application of biomacromolecule-based therapeutics is hampered by their poor cellular uptake due to poor membrane permeability [28]. As BA possesses a high affinity to saccharides, which are abundantly found on the cell surface, it was then reasoned that BA-modified biomacromolecules could be internalized on the cell surface, and subsequently cellular uptake would be enhanced. To establish the proof of concept, Ellis and co-workers chemically modified bovine pancreatic ribonuclease (RNase A) with benzoxaborole, which showed high affinity to N-acetylneuraminic acid ($Ka = 43$ M^{-1}) [29]. The subsequent cellular uptake experiment in Chinese hamster ovary cells (Lec-2) and their progenitor

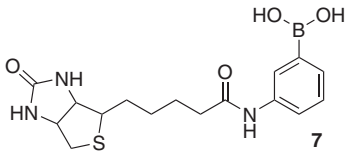

Figure 8 Biotinylated PBA **7**.

line (Pro-5) confirmed that the benzoxaborole-modified RNase A **8** showed a much higher level of cellular uptake (4–5-fold) compared to its unmodified counterpart. Meanwhile, such enhancement was abolished by the addition of D-fructose, which would competitively bind to benzoxaborole, leading to decreased binding of modified RNase A on the cell surface (Figure 9). These results demonstrated that enhanced cellular uptake is mediated by the binding between benzoxaborole and saccharides on the cellular surface. However, one possible limitation for such a strategy is that the chemical modification could affect the activity of RNase A, and the experimental results indeed showed that benzoxaborole-modified RNase A **8** only retained 17% of its ribonucleolytic activity. To mitigate such a limitation, Raines and co-workers developed a traceless system for the delivery of biological macromolecules into the cell [30]. In such a system, the benzoxaborole was ligated to the macromolecule through a self-immolative linker (trimethyl lock system) with an esterase-sensitive ester bond. The benzoxaborole moiety enhanced the uptake of the whole molecule; then, the liable ester bond was cleaved in the presence of cellular esterase, followed by the intramolecular lactonization to release the cargo (Figure 10). The initial assessment using green fluorescence protein (GFP) as the payload confirmed that the benzoxaborole-modified delivery system **9a** enhanced the cellular uptake of GFP, while the control system without the benzoxaborole moiety **9b** showed no improvement in uptake compared to GFP alone. Later, such a system was used to deliver an enzymic cytotoxin, the G88R variant of RNase A. Incubation of compound **9a** with CHO K1 cell lysates confirmed that such modification is bio-reversible, which means the free RNase A was released intact after cleaving the ester bond. An anti-proliferative assay also confirmed that compound **9a** exhibited slightly higher cytotoxicity to K-562 cells [half maximal inhibitory concentration (IC_{50}) = 3.4 μM] than the unmodified RNase A did (IC_{50}=6.5 μM), which was attributed to the benzoxaborole-mediated enhanced cellular uptake of RNase A. Such a system showed potential for the delivery of other biomacromolecules for disease treatment. It can be envisioned that this strategy could also be used to facilitate the cellular uptake of non-permeable small-molecule therapeutics.

Another therapeutic application based on carbohydrate recognition is the development of BA-containing reagents (mostly polymer-based) for the inhibition of virus replication. The infection of a host cell by viruses normally involves the interaction between some glycoproteins of the virus and their respective receptors on the host cell surface. It was then reasoned that the entry of a virus can be blocked by using synthetic receptors for the glycoproteins of the virus, which can tightly bind to the glycoproteins (e.g. gp 120 for HIV) to render the virus inactive. Because BA possesses a high affinity to saccharides, BA-modified agents are expected to show a high tendency to bind to the glycoproteins required for viral infections. Therefore, efforts were made to screen BA-containing small molecules for the inhibition of HIV viral infection. However, the monovalent PBA derivatives screened did not present any anti-HIV activities [31]. This is understandable because monovalent bonding is not strong enough to inhibit the interaction between

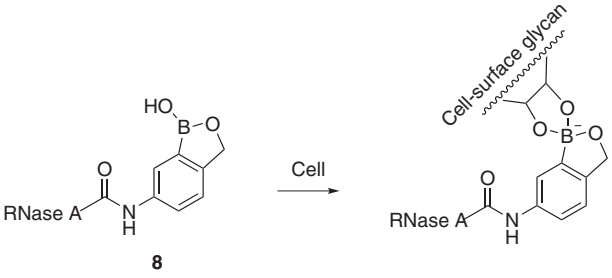

8

Figure 9 Benzoxaborole-modified RNase A **8** and its putative mechanism for expediting cellular delivery.

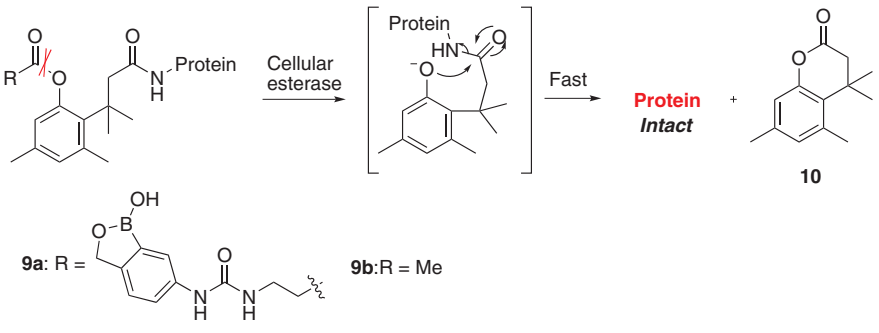

Figure 10 The strategy of intracellular traceless delivery of protein using a 'trimethyl lock' system.

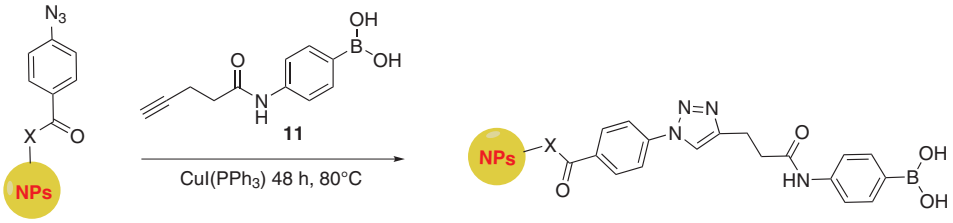

NPs: Iron-oxide-, silica- or diamond-derived

Figure 11 The BA-modified NPs for the inhibition of HCV virus entry.

viral glycoproteins and host receptors. Normally, the interface of protein-protein interactions is large and shallow. Therefore, it is not surprising that small-molecule monovalent PBA derivatives are ineffective against HIV. Consequently, multivalent binding was considered to inhibit viral entry by binding to viral glycoproteins. Several BA-modified polymers with the capacity of multivalent binding were prepared and shown to exhibit pronounced inhibition of viral entry *in vitro*, including HIV and HCV [32–34]. For example, Szunerits and co-workers ligated multi-copies of PBA to either iron oxide-, silica- or diamond-derived NPs by a Cu(I) catalyzed click reaction (Figure 11) [34]. All these three types of NPs showed very pronounced HCV entry inhibition activities, with the BA-modified silica NPs inhibiting 60 ± 8% HCV entry at a concentration of 60 μg/mL. Meanwhile, neither the unmodified NPs nor the BA derivative **11** showed any inhibition activity. These results highlighted the key role of multivalent binding in achieving the desired inhibition of viral entry.

Therapeutics based on binding to a biological target

The use of boron-based molecules for disease treatment is largely based on its carbon mimicry and ability to form covalent bonds with nucleophiles, which allow properly designed boron-containing molecules to tightly bind to biological targets. Specifically, the covalent bond formation part is especially important in the inhibition of hydrolytic enzymes, which can form a covalent complex with the BA group through the functional nucleophile or other structural Lewis base functional groups. Recent years have seen very important progress in this area with the US FDA approval of Anacor's tavaborole and crisaborole as seminal moments after the approval of bortezomib, an anticancer drug. The discussions below are either categorized based on disease implications or the specific biological targets.

Inflammation

Chemokine receptors such as CXCR1 and CXCR2 are G protein-coupled receptors (GPCR), playing a crucial role in the development of inflammation and cancer. Maeda and co-workers designed various *S*-substituted nicotinamide derivatives as potential inhibitors of chemokine CXCL1-stimulated Ca^{2+} flux in isolated human neutrophils [35]. Among the series, compound **12** (Figure 12) with a BA in the structure exhibited the most potent dual CXCR2/1 antagonist activity. It inhibited CXCL1- and CXCL8-induced Ca^{2+} flux having IC_{50} values of 38 and 36 nM, respectively. Compound **12** also significantly reduced the total cell count *in vivo* murine model of inflammation after an i.v. administration at a dose of 0.2 mg/kg, demonstrating its potent effect on inflammation. Further, oral bioavailability improvement work for such compounds was said to be in progress [35].

Anacor Pharmaceuticals has described a large pool of therapeutically active benzoxaborole analogs including AN2690 (tavaborole) for onychomycosis, AN2728 (crisaborole) for atopic dermatitis and psoriasis and AN3665 (epetraborole) for Gram-negative bacteria with good tolerability in humans. Among these agents, crisaborole (**13**) (Figure 13) is a boron-based benzoxaborole derivative, which selectively inhibits phosphodiesterase 4

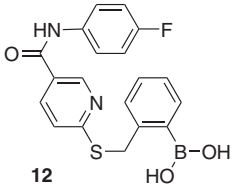

Figure 12 BA bearing an *S*-substituted nicotinamide derivative **12**.

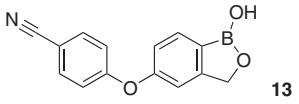

13

Figure 13 Structure of crisaborole (**13**, AN2728).

(PDE-4); thereby elevating the level of 3′,5′-cyclic adenosine monophosphate (c-AMP) at the site of inflammation. Crisaborole (**13**) further inhibits the release of three major cytokines involved in the inflammation pathway such as tumor necrosis factor-α (TNF-α), interleukins (IL-2 and IL-5) and interferon-γ (IFN-γ) [36]. In December 2016, the US FDA approved a crisaborole 2% ointment (trade name: eucrisa) for topical administration in patients suffering with eczema (atopic dermatitis) having age >2 years [37].

Akama and co-workers at Anacor Pharmaceuticals screened a library of benzoxaborole compounds (Figure 14) against IL-6, TNF-α and IL-1β and identified two lead compounds **14** and **15** with IC_{50} from 0.28 μM to 1.6 μM against IL-6, TNF-α and IL-1β. Structure-activity relationship (SAR) studies further indicated that the primary aminomethyl group is essential for inhibitory activity. Based on SAR, a series of modified compounds was synthesized and evaluated against various inflammatory cytokines. Within the series, compounds **16** and **17** exhibited good inhibitory activity against IL-6, TNF-α and IL-1β (IC_{50} from 33 to 83 nM). Compound **17** (AN3485) with an *ortho*-chloro substitution with good pharmacokinetic properties has been identified as a potential compound for clinical development for the treatment of inflammation. The mechanism of action for compound **17** is yet to be worked out [38].

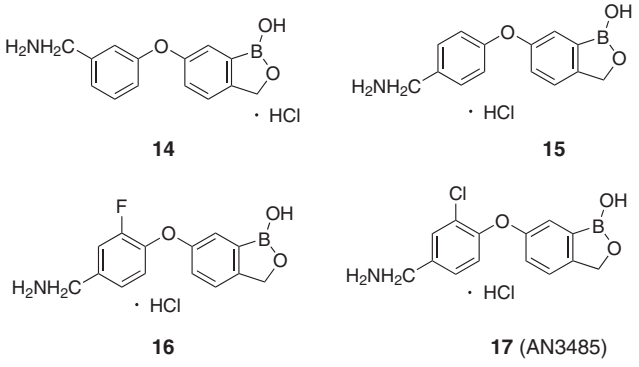

Figure 14 Structures of benzoxaborole derivatives **14–17**.

In the same year, in search of orally active anti-inflammatory agents via library screening, Akama and co-workers discovered compound **18** with IC_{50} values ranging from 2.1 to 7.2 μM and compound **19** (Figure 15) with IC_{50} values between 0.19 and 0.50 μM against IL-6, TNF-α and IL-1β [39]. The compound demonstrated low clearance and excellent bioavailability along with the inhibition of IL-6 and TNF-α elevation caused by lipopolysaccharide (LPS), after oral administration. This compound also improved collagen-induced arthritis in mice models. Compound **19** (AN4161) was considered as a potential lead molecule for the treatment of inflammation with an excellent pharmacokinetic profile [39].

Fungal infection

Anacor Pharmaceuticals discovered another benzoxaborale compound, tavaborole (**20**, AN2690) (Figure 16), which demonstrated usefulness in onychomycosis, a fungal infection of fingernails and toenails [40]. It inhibits an enzyme known as cytosolic leucyl-transfer RNA (tRNA) synthetase via the oxaborole tRNA trapping, which plays a key role in fungal essential protein synthesis [41]. US FDA approved tavaborole (**20**) for the treatment of onychomycosis in July 2014 [42].

Bacterial infection

Hernandez and co-workers discovered another aminomethyl-substituted benzoxaborole molecule, epetraborole (**21**, AN3665) (Figure 17), which is active against Gram-negative bacteria. It acts by inhibiting bacterial leucyl-tRNA synthetase, thereby proving its effectiveness in Gram-negative bacteria such as *Pseudomonas aeruginosa* and *Escherichia coli* [43]. Epetraborole was shown to be safe and without serious side effects in Phase I clinical

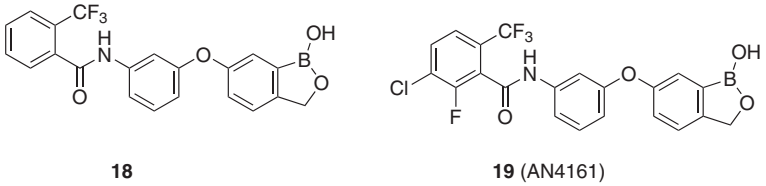

Figure 15 Structures of benzoxaborole derivatives **18** and **19**.

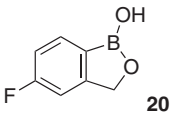

Figure 16 Structure of tavaborole (**20**, AN2690).

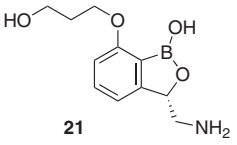

Figure 17 Structure of epetraborole (**21**, AN3665).

trials. GalaxoSmithKline then took over the clinical development of **21** (AN3365) as GSK2251052 against resistant Gram-negative bacteria. However, despite potency against Gram-negative bacterial strains, the compound was withdrawn from the second stage of clinical trials due to rapid resistance developed by the bacteria [44].

Hecker and co-workers initiated a program to discover potent inhibitors of β-lactamases to target resistant Gram-negative bacteria and to overcome the poor activity of currently marketed β-lactamase inhibitors against serine carbapenemases. Based on molecular modeling, compounds bearing a cyclic α-acylaminoboronic acid were designed on the hypothesis that intramolecular formation of a boronic ester ring would constrain the inhibitor into the preferred conformation for binding and potency enhancement. Among the synthesized compounds, vaborbactam (**22**, RPX7009) (Figure 18) emerged as the most potent compound in this series with good pharmacokinetic profiles and consistent potentiation against strains with high minimum inhibitory concentrations (MICs) to the carbapenems alone. Toxicology studies

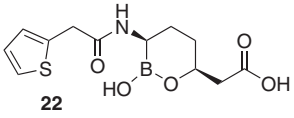

Figure 18 Structure of vaborbactam (**22**, RPX7009).

further indicated that the compound is safe at a dose of 1000 mg/kg/day with no adverse effect [45]. In Phase III clinical trials, vaborbactam in combination therapy with meropenem proved therapeutically useful in combating complicated urinary tract infections (cUTIs) [46]. In February 2017, the US FDA accepted the new drug application (NDA) filing of carbavance (a combination of vaborbactam with meropenem) for priority review for the treatment of cUTIs [47].

BA is well known to form cyclic esters with diol functionalities of sugars, thereby improving their lipophilicity and thus promoting their transport across biological lipophilic membranes. Bandyopadhyay and co-workers reported a series of 2-acetylphenylboronic acids bearing a typical amino acid. 2-Acetylphenylboronic acid selectively couples with the nucleophilic amino functionality present in the lipid membrane layer of bacterial cells such as phosphatidylethanolamine (PE) and phosphatidylglycerol (PG) via formation of iminoboronates. Cysteine methyl ester (Cys-OMe) was used as a linkage to link 2-APBA with amine-reactive fluorophores such as a fluorescein isothiocyanate (Figure 19). The resulting fluorescent-labeled 2-APBA (**23**) showed significant association with lipid vesicles compared to similar compound **24**, which lacks BA, thereby demonstrating the significance of the BA unit in activating the ketone functional group for a condensation reaction with the amino group of PE or PG. Compound **23** selectively stains Gram-positive bacterial strains but is unable to strain Gram-negative organisms, probably due to the absence of PG or PE in the outer layer of *E. coli* and mammalian cells. Conjugating **23** and peptides further improves its activity for tagging the bacteria and minimizing the effect of serum proteins due to its affinity towards bacteria. The results demonstrated excellent selectivity of **23** against bacteria even in the presence of serum protein [48].

Reddy and co-workers further designed a strategy to develop effective antimicrobial compounds by combining boron with carbohydrates and imines [49]. They reported the synthesis of 24 boronic ester derivatives with xylofuranose as carbohydrate components. These compounds were tested against various microbial strains for

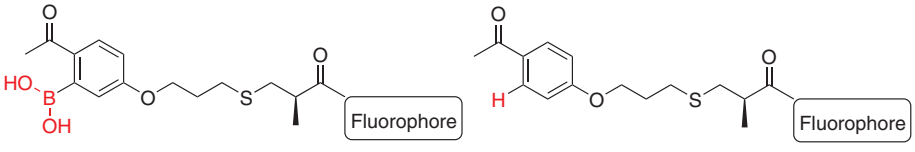

Figure 19 Structures of compounds **23** and **24** with a conjugated fluorophore.

their antifungal and antibacterial activities, and exhibited good-to-moderate *in vitro* activity against fungal as well as both Gram-positive and Gram-negative strains. Among various compounds, **25** (Figure 20) emerged as a potent inhibitor of all microbial strains used in the assay [50].

Pain treatment

Selective targeting of the fatty acid amide hydrolase (FAAH) pathway emerged as a promising approach for the treatment of inflammation and pain. Arylboronic acids were reported by several researchers as potent selective inhibitors of the FAAH pathway, and can be used for relief from pain [51]. PF-04457845, one of the selective FAAH inhibitors that entered clinical trials for analgesic activity, was withdrawn from Phase II clinical trials due to poor efficacy, despite evidence of peripheral target engagement [52]. The failure of PF-04457845 was attributed to triggering transient receptor potential vanilloid 1 (TRPV1), which is responsible for pain development. TRPV1, a channel-based cationic pathway, also emerged as a validated approach for analgesic and anti-inflammatory therapy. Therefore, developing dual inhibitors of TRPV1 and FAAH may be useful for pain therapy [53]. In 2016, Morera and co-workers reported a series of 31 compounds by incorporation of BA (FAAH-inhibiting scaffold) in the reported TRPV1 antagonists to develop dual inhibitors of FAAH and TRPV1. Among the series, four compounds **26–29** (Figure 21) acted as potent dual inhibitors having IC_{50} values from 0.56 to 8.11 μM. These compounds simultaneously inhibit two distinct targets and thus qualify as promising antinociceptive, antihyperalgesic and antiedemic agents [54].

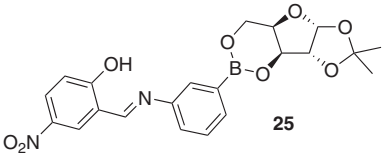

Figure 20 Structure of compound **25**.

Cancer

Fulvestran (**30**) is the only FDA-approved selective estrogen receptor downregulator (SERD) used clinically for the management of metastatic breast cancer. It has poor bioavailability and requires 3 months to reach steady-state serum concentration [55]. It undergoes rapid and extensive O-glucuronidation and O-sulfation to form polar Phase II metabolites that are inactive and water-soluble. Further, sulfotransferases catalyze sulfate conjugation with fulvestrant at the C-3 position, leading to rapid excretion of fulvestrant as a sulfate conjugate from systemic circulation. Metabolic studies proved that the -OH at the C-3 position of fulvestrant is vulnerable to first-pass metabolism [56]. Liu and co-workers extensively studied the metabolic pathway of fulvestrant and modified the -OH at C-3 with BA to yield a potent and orally bioavailable fulvestrant-3-BA (**31**) (Figure 22). Structural modification on the C-3 position of fulvestrant by introducing a BA moiety leads to blockage of first-pass metabolism while retaining major characteristics of the SERD. This highly orally bioavailable fulvestrant-3-BA as an effective steroidal oral SERD may be useful in patients with ER-positive endocrine-resistant breast cancer [57].

Tamoxifen, a clinically used drug, is an inactive precursor, which metabolizes in the body into its biologically active form 4-hydroxytamoxifen (4-OHT) by the cytochrome P450 enzyme. Tamoxifen is used clinically for the treatment of breast cancer. 4-OHT has poor bioavailability due to rapid first-pass clearance. Zhong and

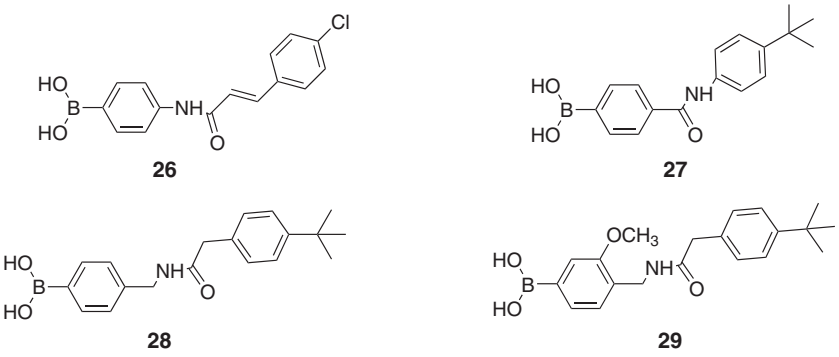

Figure 21 Structures of compounds **26–29**.

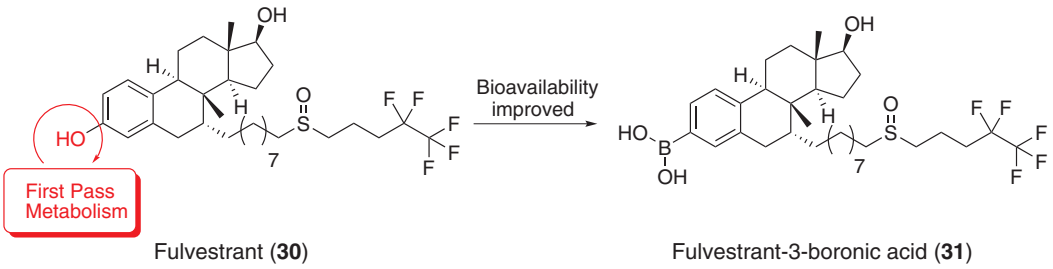

Figure 22 Bioavailability improvement of fulvestrant (**30**) by incorporation of BA.

co-workers designed a boronic prodrug of 4-OHT (**32**) (Figure 23), with the aim of enhancing its potency along with reducing the dosage to minimize the side effects associated with it. The prodrug **32** demonstrated excellent bioavailability compared to tamoxifen in various models of breast cancer [58].

Reddy and co-workers reported the synthesis of various boronate ester complexes of palladium with pyridyl-imine and diols such as mannitol and xylose. These compounds were screened against breast cancer and human colon cancer cell lines. All compounds demonstrate good-to-moderate activity, having IC_{50} values from 4.27 to 34.76 μM against both cancer cell lines. Among the series, compound **33** emerged as a potent and selective inhibitor against colon cancer and breast cancer cell lines, with IC_{50} values of 6.71 and 8.58 μM, respectively. Further, compound **34** was found to be more toxic (2-fold) compared to cisplatin in colon cancer cells lines. These complexes (Figure 24) were also tested on human embryonic non-tumorigenic kidney cells, showing less toxicity. Further, compounds without the boronic ester exhibit poor activity in cancer cell lines, demonstrating the significance of boronic ester in selectively targeting the cancer cell lines. Further studies showed that these compounds intercalate into DNA [49].

Canturk and co-workers studied the usefulness of sodium tetraborate and boric acid on human promyelocytic leukemia cells and healthy human lymphocyte cells. Using the MTT assay, both compounds reduced the mitochondrial activity in cell lines at the highest concentration, 1000 μM. The activity of promyelocytic leukemia cells

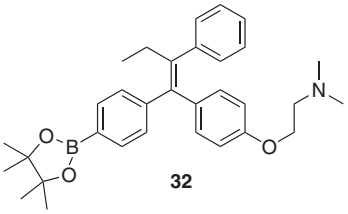

Figure 23 BA-based prodrug of 4-OHT (**32**).

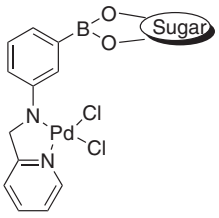

Figure 24 Boronate ester complex of palladium **33** (sugar: 1,2-O-isopropylidene-α-D-xylofuranose) and **34** (sugar: 1,2:5,6-di-O-isopropylidene-D-mannitol).

was found to be significantly reduced even at 100 μM after an incubation period of 48 h ($p < 0.001$). Boric acid also proved to have high lysosomal activity on leukemia cells while in the case of sodium tetraborate, a 4% decrease was noticed. Boric acid also proved to be more effective on leukemia cells in producing apoptosis (4-fold) compared to lymphocytes. Transmission electron microscopy (TEM) results further showed that boric acid also stimulates extra nucleus formation in both the cell lines (at 100 μM). Therefore, boric acid proved to be more cytotoxic on leukemia cells in comparison to healthy lymphocytes and the mitochondrial pathway than sodium tetraborate [59].

Ocular delivery

Liu and co-workers modified conventional cyclosporine A NPs with PBA to achieve mucoadhesive properties for the sustained delivery of cyclosporine in the treatment of anterior eye disease such as dry eye syndrome [60]. The mucoadhesion properties of NPs with pendent PBA interact with the diol functionality of carbohydrates present on the surface of mucin (Figure 25). These modified mucoadhesive NPs loaded with cyclosporine at very high concentrations increase the retention of drug in the eye due to the muchoadhesive characteristic, and effectively deliver cyclosporine for long durations in the eye. Therefore, the mucoadhesive dosage form could help reduce the adverse effect associated with frequent dosing or missing doses

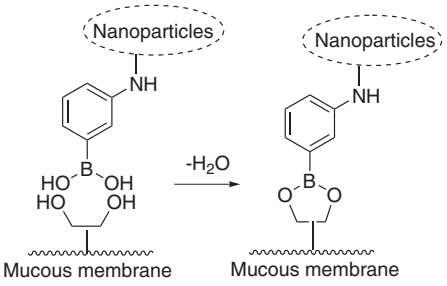

Figure 25 Interaction of PBA-modified NPs with the cis-diol group on the surface of mucin.

in dry eye syndrome or other disorders. Cyclosporine A-loaded PBA NPs further eliminate the inflammatory infiltrates along with complete restoration of the ocular surface [60].

Enzyme inhibitors

Hormone-sensitive lipase inhibitors

Numerous studies in the past reported BA molecules as potent reversible and selective inhibitors of hormone-sensitive lipase (HSL) [61, 62]. However, no potency data was available for these compounds. Ogiyama and co-workers designed a series of reversible inhibitors of HSL having both a hydrophobic center as well as an electrophilic center [63]. Among the various compounds in the series, BA-bearing compound **35** (Figure 26) exhibited excellent inhibitory activity (IC_{50} value of 7 nM) against HSL. Kinetic studies revealed that compound **35** showed a mixed type inhibition, indicating it binds directly to enzyme (HSL) as well as to enzyme (HSL)-substrate complex. Experimental results further confirmed significant binding of compound **35** with HSL [63].

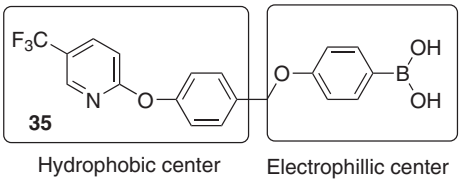

Figure 26 Structure of compound **35**.

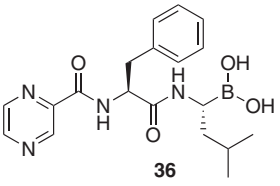

Figure 27 Structure of bortezomib (**36**).

Proteasome inhibitors

Bortezomib (**36**), a dipeptide BA (Figure 27), is a selective first-generation proteasome inhibitor, clinically used in patients with multiple myeloma (MM) [64, 65]. Although having significant potency, clinical utility of bortezomib (**36**) is limited due to its adverse effects and rapid resistance developed during therapy [63].

Based on the importance of BA in proteasome inhibition as in the case of bortezomib, researchers at Takeda Oncology discovered ixazomib citrate (**37**, MLN9708), a boronic ester-based peptidic orally bioavailable, potent, selective proteasome inhibitor [66, 67]. It rapidly hydrolyzes in plasma to its biological active form ixazomib (**38**, MLN 2238) (Figure 28). Ixazomib selectively targets the proteasome by inhibiting its chymotrypsin activity (IC_{50} value of 3.4 nM) [68]. It also demonstrated faster proteasome dissociation half-life ($t_{1/2}$ = 18 min) compared to bortezomib ($t_{1/2}$ = 110 min). Oral and intravenous administrations of ixazomib significantly inhibited MM tumor growth ($p = 0.001$) in tumor-bearing mice and prolonged survival (87%; $p < 0.001$) of these mice [68, 69]. On 20 November 2015, the US FDA approved ixazomib (ninlaro) for the patients with MM in combination with dexamethasone and lenalidomide [70].

Milani and co-workers further reported the design, synthesis and screening of a series of BAs as proteasome inhibitors. Among the series, a boronic ester derivative

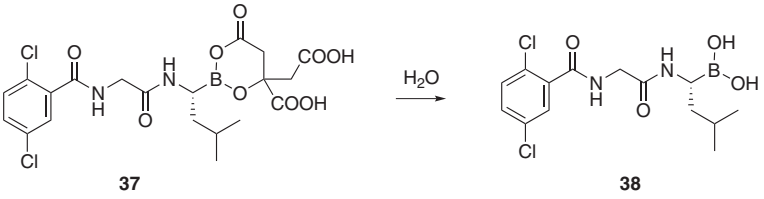

Figure 28 Hydrolysis of ixazomib citrate (**37**) to the biologically active form ixazomib (**38**).

with an *S*-benzylcysteine-(3-phenyl) substituent (**39**) (Figure 29) showed potent inhibition of proteasome chymotrypsin activity, having an IC_{50} value of 52 μM [71]. Momose and co-workers previously identified tyropeptins and tyropeptin-BA as potent proteasome inhibitors, with IC_{50} values of 0.14 and 0.0063 μM, respectively, against chymotrypsin-like (CT-L) activity of the 20S proteosome [72, 73]. Based on previous results and SAR information, they designed two potent tyropeptin-BA derivatives **40** and **41** (Figure 30) with IC_{50} values of 0.014 and 0.0022 μM, respectively [74]. Both **40** and bortezomib (IC_{50}=0.0094 μM) inhibit CT-L activity of the 20S proteasome with almost equal potency, but compound **41** emerged as a more potent inhibitor compared to bortezomib. Due to low permeation in tumors, compound **41** was found to be less potent in tumor proteasome inhibition as well as in suppressing the growth of tumors in mice bearing human MM compared to compound **40**. Therefore, compound **40** is considered as a lead structure for further optimization to develop new molecules in the treatment of MM [74]. In search for a safer alternative to bortezomib, Shi and co-workers designed a new series of proteasome inhibitors bearing both peptidic as well BA domains similar to bortezomib (**36**), along with αα-/αβ-amino acids and substitution in place of the pyrazine ring of bortezomib (Figure 31).

Compounds composed of αα-amino acids retained activity while compounds with αβ-amino acids **42** lost activity completely. Among the αα-amino acids series, compound **43** emerged as the lead proteasome inhibitior with an excellent IC_{50} value (4.82 nM) along with the highest potency against MM cell lines with IC_{50} values less than 10 nM. Molecular docking studies showed that compound **43** occupies the β5 subunit active pocket of the proteasome similar to that of bortezomib (**36**) [75].

Because of the immunogenicity and poor metabolic stability and poor membrane permeability of peptidic drugs such as bortezomib (**36**), Ge and co-workers synthesized and evaluated new proteasome inhibitors bearing non-peptidic BA along with a 1,4-naphthoquinone scaffold (Figure 32). The compounds showed promising inhibition against the 20S proteasome with compound **44** having an IC_{50} value of 11.4 nM, which is comparable to that of bortezomib (**36**). In a cellular proliferation inhibition assay, compound **44** demonstrated excellent anti-proliferative activities against solid tumor cell lines along with much improved metabolic stability compared to bortezomib (**36**). Compound **44** can be used as a lead for the future development of non-peptidic proteasome inhibitors [76].

Histone deacetylase inhibitors

Islam and co-workers designed BA-based bicyclic tetrapeptides (Figure 33) as selective inhibitors of histone deacetylase (HDAC) using BA as the zinc (Zn)-binding domain. Compounds **45** and **46** contain the same scaffold with different Zn-binding domains. However, the BA-derivative **45** showed very poor potency (IC_{50} = 12 000 nM and 10 000 nM in two assays) compared to methoxymethyl ketone-based compound **46** (IC_{50} = 27 nM and 32 nM) [77].

Neuroprotective activity

Alzheimer's disease

BA derivatives were described by various researchers for their usefulness in the treatment of Alzheimer's disease (AD) via inhibition of various serine proteases such as thrombin and prolyl oligopeptidases along with autotaxin, an enzyme expressed in AD. Jiménez-Aligaga and co-workers reported a new series of BA and boronate esters targeting various pathways involved in the pathogenesis

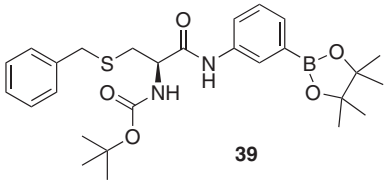

39

Figure 29 Structure of compound **39**.

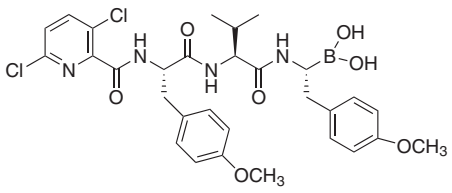

40

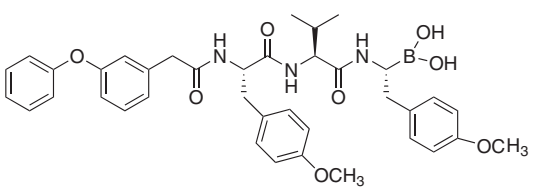

41

Figure 30 Structures of compounds **40** and **41**.

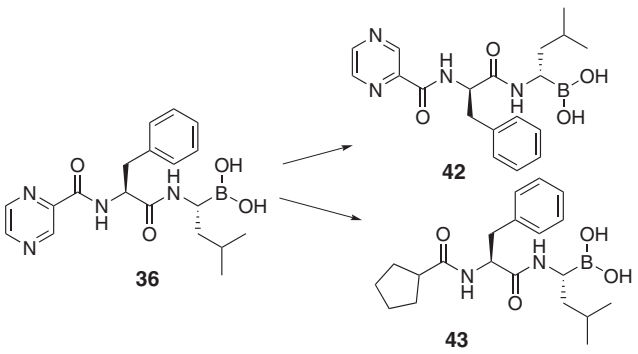

Figure 31 Chemical modifications of bortezomib (**36**) to compounds **42** and **43**.

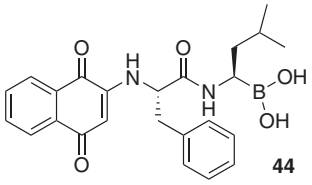

Figure 32 Structure of non-peptidic BA with a 1,4-naphthoquinone scaffold (**44**).

of AD. Compound **47** (Figure 34) was highly active in lowering malondialdehyde (MDA) level (36 nmol/mg protein), which may be responsible for nerve cell dysfunction in neurological disorders. Compound **47** also caused enhancement of the glutathione/glutathione disulfide (GSH/GSSG) ratio due to an increased GSH level (32 nmol/mg protein), which plays a crucial role in neuroprotection from reactive oxygen species (ROS). Compound **47** further showed potent activity against generation of ROS with an IC_{50} value of 2.85 μM. Further, compound **47** reduced the level of caspase 3, thereby making it an attractive compound to be highly useful in neuroprotection [78].

Jung and co-workers reported various chalcone-based BA fluorescent probes for the detection of β-amyloid plaques from AD. They envisioned that BA in the probe can form a strong bond with amino acid residues of β-amyloid plaques. Compound **48** (Figure 35) exhibited a significant improvement in fluorescence in the synthetic β-amyloid aggregates for their fluorescence responses. Due to the presence of BA, compound **48** effectively binds to β-amyloid aggregates ($K_D = 0.79 \pm 0.05$ μM). Compound **48** selectively stained β-amyloid in the brains of experimental mice. Studies in mouse models further revealed that compound **48** has sufficient lipophilicity to cross the blood-brain barrier (BBB) and causes staining of amyloid plaques. It was proposed that compound **48** with a BA functional group may prove to be a good sensor to study neuronal functions in AD [79].

Amyotrophic lateral sclerosis

Amyotrophic lateral sclerosis (ALS), a neurodisorder caused by the selective destruction of nerve cells in the brain and spinal cord, is due to oxidative stress. ALS is a disease resulting from defective mutation of the human gene encoding the secretory RNase angiogenin (ANG). Hoang and co-workers reported a synthetic BA mask (**49**, Figure 36) that restrains the ribonucleolytic activity of ANG as it relies on the intracellular manifestation of ANG's ribonucleolytic activity to mediate neuroprotection. Hydrogen peroxide (H_2O_2) causes oxidative cleavage of the boron-carbon bond in PBA thereby releasing the active ANG preferentially only in cells suffering from ROS-mediated toxicity. Compound **49** is inactive under normal physiological conditions, while it becomes active in the presence of the most prevalent ROS, H_2O_2 [80].

Boron neutron capture therapy

BNCT is a radiotherapy used clinically for the management of various cancers. BNCT relied on targeted delivery of ^{10}B in the tumor cells, which on irradiation with low-energy neutrons decays into very toxic ^{7}Li and ^{4}He ions. These toxic ions cause the selective destruction of the

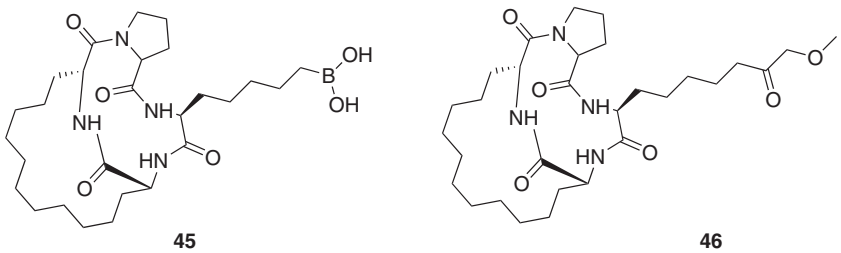

Figure 33 BA-based bicyclic tetrapeptides **45** and **46**.

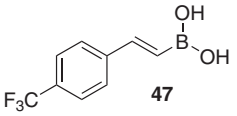

Figure 34 Structure of compound **47**.

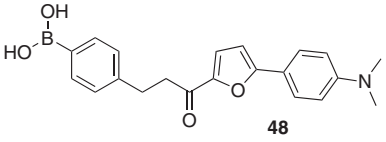

Figure 35 Chalcone-based BA fluorescent probe **48**.

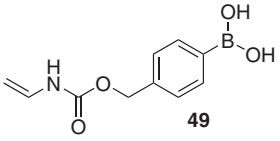

Figure 36 Structure of compound **49**.

closest neighboring cells at the site of their production. Borocaptate (BSH) and 4-dihydroxyborylphenylalanine (BPA) have proven to be selective BNCT carriers to target tumor cells compared to others compounds such as boric acid, sodium borate, sodium pentaborate and polyhedral borane anions (GB-10). However, both BSH and BPA have achieved limited successes in clinical trials, probably due to the very low penetration of boron into the tumor compared to high concentrations in the blood [81].

Achilli and co-workers reported a series of PBA conjugates with folic acid (FA) illustrated by compound **50** (Figure 37) as BNCT with the assumption that FA-conjugated molecules could selectively deliver ^{10}B into cancer cells. Compound **50** produces significant inflammation and thrombotic effects, which discourages the potential applications of these molecule in BNCT. Conversely, compound **50** has good biocompatibility with blood cells. Therefore, it can be considered as a lead for the development of safer BNCT carriers for selectively targeting tumor cells without affecting normal blood cells [82].

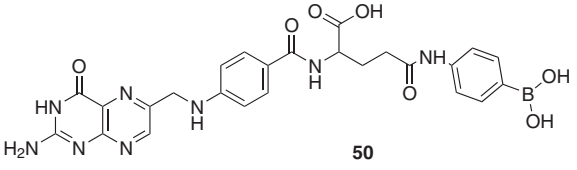

Figure 37 PBA conjugate with folic acid (**50**) for BNCT.

Hattaori and co-workers at the Research Center of Boron Neutron Capture Therapy, Osaka Prefecture University, Japan, developed a fluorescent sensor DAHMI (**51**) for the detection of boron-based pharmaceuticals. DAHMI reacted rapidly (within 20 min) with BA in aqueous media, resulting in the emission of blue fluorescence due to the formation of the DAHMI-BA complex **52** (Figure 38) in live tumor B16 cells at 0.5–1 mM concentration. Furthermore, DAHMI passes through the cell membranes; thus, it can be used to visualize BA distribution in immobilized cells without requiring prior cell permeabilization. Using this probe, it was shown that both BPA and fluorinated BPAs are distributed throughout the cell, while tavaborole and PBA are distributed in the cytosol but excluded from the cell nucleus. These results demonstrated the utility of DAHMI as a tool to assess the distribution of BA derivatives in live cells [83, 84].

Conclusion

The last decade has witnessed a significant expansion in the applications of boron-based molecules in therapeutic areas, with the approval of ixazomib, tavaborole and crisaborole as milestone moments. At the same time, there have also been continuous efforts in using BA for sugar sensing. Given the special properties of boron in its ability to mimic carbon and bind with nucleophiles and Lewis bases, we hope to see an accelerated pace of research in the biological application of boron-containing compounds.

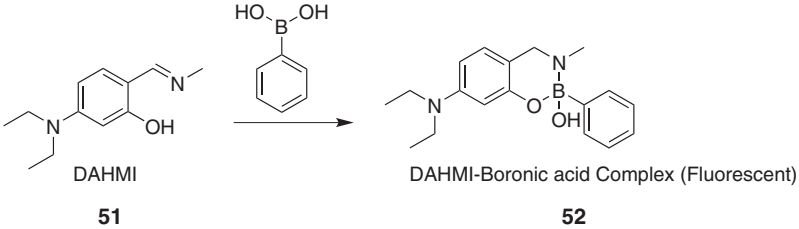

Figure 38 Reaction of fluorescent sensor DAHMI (**51**) with BA produces a fluorescent DAHMI-BA complex (**52**).

References

[1] Yang, W.; Gao, X.; Wang, B. Boronic acid compounds as potential pharmaceutical agents. *Med. Res. Rev.* **2003**, *23*, 346–348.

[2] Zhai, W.; Sun, X.; James, T. D.; Fossey, J. S. Boronic acid-based carbohydrate sensing. *Chem. Asian J.* **2015**, *10*, 1836–1848.

[3] Jin, S.; Cheng, Y.; Reid, S.; Li, M.; Wang, B. Carbohydrate recognition by boronolectins, small molecules, and lectins. *Med. Res. Rev.* **2010**, *30*, 171–257.

[4] Fang, H.; Kaur, G.; Wang, B. Progress in boronic acid-based fluorescent glucose sensors. *J. Fluoresc.* **2004**, *14*, 481–489.

[5] Wu, X.; Li, Z.; Chen, X. X.; Fossey, J. S.; James, T. D.; Jiang, Y. B. Selective sensing of saccharides using simple boronic acids and their aggregates. *Chem. Soc. Rev.* **2013**, *42*, 8032–8048.

[6] Galbraith, E.; James, T. D. Boron based anion receptors as sensors. *Chem. Soc. Rev.* **2010**, *39*, 3831–3842.

[7] Yan, J.; Fang, H.; Wang, B. Boronolectins and fluorescent boronolectins: an examination of the detailed chemistry issues important for the design. *Med. Res. Rev.* **2005**, *25*, 490–520.

[8] Cao, H.; Heagy, M. D. Fluorescent chemosensors for carbohydrates: a decade's worth of bright spies for saccharides in review. *J. Fluoresc.* **2004**, *14*, 569–584.

[9] Ni, N.; Wang, B. Applications of boronic acids in chemical biology and medicinal chemistry. In *Boronic Acids*. Wiley-VCH Verlag GmbH & Co. KGaA: Weinheim, Germany, 2011, pp 591–620.

[10] Heagy, M. D. N-Phenylboronic acid derivatives of arenecarboximides as saccharide probes with virtual spacer design. *Topics in Fluorescence Spectroscopy,* Springer Science (USA), **2006**, Vol. 11, pp 1–20.

[11] Arnaud, J.; Audfray, A.; Imberty, A. Binding sugars: from natural lectins to synthetic receptors and engineered neolectins. *Chem. Soc. Rev.* **2013**, *42*, 4798–4813.

[12] Mergenthaler, P.; Lindauer, U.; Dienel, G. A.; Meisel, A. Sugar for the brain: the role of glucose in physiological and pathological brain function. *Trend. Neurosci.* **2013**, *36*, 587–597.

[13] Raddatz, D.; Ramadori, G. *Z.* Carbohydrate metabolism and the liver: actual aspects from physiology and disease. *Gastroenterol.* **2007**, *45*, 51–62.

[14] Sairam, M. R. Role of carbohydrates in glycoprotein hormone signal transduction. *FASEB J.* **1989**, *3*, 1915–1926.

[15] Stowell, S. R.; Ju, T.; Cummings, R. D. Protein glycosylation in cancer. *Annu. Rev. Pathol.* **2015**, *10*, 473–510.

[16] Yan, J.; Springsteen, G.; Deeter, S.; Wang, B. The relationship among pKa, pH, and binding constants in the interactions between boronic acids and diols – it is not as simple as it appears. *Tetrahedron* **2004**, *60*, 11205–11209.

[17] Springsteen, G.; Wang, B. A detailed examination of boronic acid–diol complexation. *Tetrahedron* **2002**, *58*, 5291–5300.

[18] Chu, Y.; Wang, D.; Wang, K.; Liu, Z. L.; Weston, B.; Wang, B. Fluorescent conjugate of sLe(x)-selective bisboronic acid for imaging application. *Bioorg. Med. Chem. Lett.* **2013**, *23*, 6307–6309.

[19] Yang, W.; Fan, H.; Gao, X.; Gao, S.; Karnati, V. V.; Ni, W.; Hooks, W. B.; Carson, J.; Weston, B.; Wang, B. The first fluorescent diboronic acid sensor specific for hepatocellular carcinoma cells expressing sialyl Lewis X. *Chem. Biol.* **2004**, *11*, 439–448.

[20] Xu, X. D.; Cheng, H.; Chen, W. H.; Cheng, S. X.; Zhuo, R. X.; Zhang, X. Z. In situ recognition of cell-surface glycans and targeted imaging of cancer cells. *Sci. Rep.* **2013**, *3*, 2679.

[21] Gao, X.; Zhu, M.; Fan, H.; Yang, W.; Ni, W.; Karnati, V. V.; Gao, S.; Carson, J.; Weston, B.; Wang, B. A fluorescent bisboronic acid compound that selectively labels cells expressing oligosaccharide Lewis X. *Bioorg. Med. Chem. Lett.* **2015**, *25*, 2501–2504.

[22] Chaudhary, P. M.; Murthy, R. V.; Yadav, R.; Kikkeri, R. A rationally designed peptidomimetic biosensor for sialic acid on cell surfaces. *Chem. Commun.* **2015**, *51*, 8112–8115.

[23] Chang, M.-H.; Chang, C.-N. Synthesis of three fluorescent boronic acid sensors for tumor marker Sialyl Lewis X in cancer diagnosis. *Tetrahedron Lett.* **2014**, *55*, 4437–4441.

[24] Culf, A. S.; Yin, H.; Monro, S.; Ghosh, A.; Barnett, D. A.; Ouellette, R. J.; Cuperlovic-Culf, M.; McFarland, S. A. A spectroscopic study of substituted anthranilic acids as sensitive environmental probes for detecting cancer cells. *Bioorg. Med. Chem.* **2016**, *24*, 929–937.

[25] Shinde, S.; El-Schich, Z.; Malakpour, A.; Wan, W.; Dizeyi, N.; Mohammadi, R.; Rurack, K.; Gjorloff Wingren, A.; Sellergren, B. Sialic acid-imprinted fluorescent core-shell particles for selective labeling of cell surface glycans. *J. Am. Chem. Soc.* **2015**, *137*, 13908–13912.

[26] Stephenson-Brown, A.; Acton, A. L.; Preece, J. A.; Fossey, J. S.; Mendes, P. M. Selective glycoprotein detection through covalent templating and allosteric click-imprinting. *Chem. Sci.* **2015**, *6*, 5114–5119.

[27] Zhang, X.; Chen, B.; He, M.; Zhang, Y.; Peng, L.; Hu, B. Boronic acid recognition based-gold nanoparticle-labeling strategy for the assay of sialic acid expression on cancer cell surface by inductively coupled plasma mass spectrometry. *Analyst* **2016**, *141*, 1286–1293.

[28] Malik, D. K.; Baboota, S.; Ahuja, A.; Hasan, S.; Ali, J. Recent advances in protein and peptide drug delivery systems. *Curr. Drug Deliv.* **2007**, *4*, 141–151.

[29] Ellis, G. A.; Palte, M. J.; Raines, R. T. Boronate-mediated biologic delivery. *J. Am. Chem. Soc.* **2012**, *134*, 3631–3634.

[30] Andersen, K. A.; Smith, T. P.; Lomax, J. E.; Raines, R. T. Boronic acid for the traceless delivery of proteins into cells. *ACS Chem. Biol.* **2016**, *11*, 319–323.

[31] Trippier, P. C.; McGuigan, C.; Balzarini, J. Phenylboronic-acid-based carbohydrate binders as antiviral therapeutics: monophenylboronic acids. *Antivir. Chem. Chemother.* **2010**, *20*, 249–257.

[32] Jay, J. I.; Lai, B. E.; Myszka, D. G.; Mahalingam, A.; Langheinrich, K.; Katz, D. F.; Kiser, P. F. Multivalent benzoboroxole functionalized polymers as gp120 glycan targeted microbicide entry inhibitors. *Mol. Pharm.* **2010**, *7*, 116–129.

[33] Mahalingam, A.; Geonnotti, A. R.; Balzarini, J.; Kiser, P. F. Activity and safety of synthetic lectins based on benzoboroxole-functionalized polymers for inhibition of HIV entry. *Mol. Pharm.* **2011**, *8*, 2465–2475.

[34] Khanal, M.; Vausselin, T.; Barras, A.; Bande, O.; Turcheniuk, K.; Benazza, M.; Zaitsev, V.; Teodorescu, C. M.; Boukherroub, R.; Siriwardena, A.; et al. Phenylboronic-acid-modified nanoparticles: potential antiviral therapeutics. *ACS Appl. Mater. Interfaces* **2013**, *5*, 12488–12498.

[35] Maeda, D. Y.; Peck, A. M.; Schuler, A. D.; Quinn, M. T.; Kirpotina, L. N.; Wicomb, W. N.; Fan, G.-H.; Zebala, J. A. Discovery of 2-[5-(4-Fluorophenylcarbamoyl)pyridin-2-ylsulfanylmethyl]phenylboronic acid (SX-517): noncompetitive boronic acid antagonist of CXCR1 and CXCR2. *J. Med. Chem.* **2014**, *57*, 8378–8397.

[36] Jarnagin, K.; Chanda, S.; Coronado, D.; Ciaravino, V.; Zane, L. T.; Guttman-Yassky, E.; Lebwohl, M. G. Crisaborole topical ointment, 2%: A nonsteroidal, topical, anti-inflammatory phosphodiesterase 4 inhibitor in clinical development for the treatment of atopic dermatitis. *J. Drugs Dermatol.* **2016**, *15*, 390–396.

[37] Timmins, P. An industry update: what are the latest developments in the field of therapeutic delivery? Industry Update: 1st December to 31st December 2016. *Ther. Deliv.* **2017**, *8*, 185–199.

[38] Akama, T.; Virtucio, C.; Dong, C.; Kimura, R.; Zhang, Y.-K.; Nieman, J. A.; Sharma, R.; Lu, X.; Sales, M.; Singh, R.; et al. Structure–activity relationships of 6-(aminomethylphenoxy)-benzoxaborole derivatives as anti-inflammatory agent. *Bioorg. Med. Chem. Lett.* **2013**, *23*, 1680–1683.

[39] Akama, T.; Dong, C.; Virtucio, C.; Freund, Y. R.; Chen, D.; Orr, M. D.; Jacobs, R. T.; Zhang, Y.-K.; Hernandez, V.; Liu, Y.; et al. Discovery and structure–activity relationships of 6-(benzoylamino)benzoxaboroles as orally active anti-inflammatory agents. *Bioorg. Med. Chem. Lett.* **2013**, *23*, 5870–5873.

[40] Baker, S. J.; Zhang, Y.-K.; Akama, T.; Lau, A.; Zhou, H.; Hernandez, V.; Mao, W.; Alley, M. R. K.; Sanders, V.; Plattner, J. J. Discovery of a new boron-containing antifungal agent, 5-fluoro-1,3-dihydro-1-hydroxy-2,1- benzoxaborole (AN2690), for the potential treatment of onychomycosis. *J. Med. Chem.* **2006**, *49*, 4447–4450.

[41] Sharma, N.; Sharma, D. An upcoming drug for onychomycosis: tavaborole. *J. Pharmacol. Pharmacother.* **2015**, *6*, 236–239.

[42] Markham, A. Tavaborole: first global approval. *Drugs* **2014**, *74*, 1555–1558.

[43] Hernandez, V.; Crépin, T.; Palencia, A.; Cusack, S.; Akama, T.; Baker, S. J.; Bu, W.; Feng, L.; Freund, Y. R.; Liu, L.; et al. Discovery of a novel class of boron-based antibacterials with activity against gram-negative bacteria. *Antimicrob. Agents Chemother.* **2013**, *57*, 1394–1403.

[44] O'Dwyer, K.; Spivak, A.; Ingraham, K.; Min, S.; Holmes, D. J.; Jakielaszek, C.; Rittenhouse, S.; Kwan, A.; Livi, G. P.; Sathe, G.; et al. Bacterial resistance to leucyl-tRNA synthetase inhibitor GSK2251052 develops during treatment of complicated urinary tract infections. *Antimicrob. Agents Chemother.* **2014**, *59*, 289–298.

[45] Hecker, S. J.; Reddy, K. R.; Totrov, M.; Hirst, G. C.; Lomovskaya, O.; Griffith, D. C.; King, P.; Tsivkovski, R.; Sun, D.; Sabet, M.; et al. Discovery of a cyclic boronic acid β-lactamase inhibitor (RPX7009) with utility vs class A serine carbapenemases. *J. Med. Chem.* **2015**, *58*, 3682–3692.

[46] Castanheira, M.; Rhomberg, P. R.; Flamm, R. K.; Jones, R. N. Effect of the β-lactamase inhibitor vaborbactam combined with meropenem when tested against serine-carbapenemase-producing enterobacteriaceae. *Antimicrob. Agents Chemother.* **2016**, *60*, 5623–5624.

[47] The Medicines Company Announces FDA Filing Acceptance of New Drug Application for Intravenous Antibiotic Carbavance® (meropenem-vaborbactam) http://www.themedicinescompany.com/investors/news/medicines-company-announces-fda-filing-acceptance-new-drug-application-intravenous (Accessed on April 05, 2017).

[48] Bandyopadhyay, A.; McCarthy, K. A.; Kelly, M. A.; Gao, J. Targeting bacteria via iminoboronate chemistry of amine-presenting lipids. *Nat. Commun.* **2015**, *6*, 6561.

[49] Reddy, E. R.; Trivedi, R.; Sarma, A. V. S.; Sridhar, B.; Anantaraju, H. S.; Sriram, D.; Yogeeswari, P.; Nagesh, N. Sugar-boronate ester scaffold tethered pyridyl-imine palladium(ii) complexes: synthesis and their *in vitro* anticancer evaluation. *Dalton Transactions* **2015**, *44*, 17600–17616.

[50] Reddy, E. R.; Trivedi, R.; Sudheer Kumar, B.; Sirisha, K.; Sarma, A. V. S.; Sridhar, B.; Prakasham, R. S. Synthesis, characterization and antimicrobial activity of novel Schiff base tethered boronate esters of 1,2-O-isopropylidene-α-d-xylofuranose. *Bioorg. Med. Chem. Lett.* **2016**, *26*, 3447–3452.

[51] Minkkilä, A.; Saario, S. M.; Käsnänen, H.; Leppänen, J.; Poso, A.; Nevalainen, T. Discovery of boronic acids as novel and potent inhibitors of fatty acid amide hydrolase. *J. Med. Chem.* **2008**, *51*, 7057–7060.

[52] Keith, J. M.; Jones, W. M.; Tichenor, M.; Liu, J.; Seierstad, M.; Palmer, J. A.; Webb, M.; Karbarz, M.; Scott, B. P.; Wilson, S. J.; et al. Preclinical characterization of the FAAH inhibitor JNJ-42165279. Preclinical characterization of the FAAH inhibitor JNJ-42165279. *ACS Med. Chem. Lett.* **2015**, *6*, 1204–1208.

[53] Kaneko, Y.; Szallasi, A. Transient receptor potential (TRP) channels: a clinical perspective. *Br. J. Pharmacol.* **2014**, *171*, 2474–2507.

[54] Morera, E.; Di Marzo, V.; Monti, L.; Allarà, M.; Schiano Moriello, A.; Nalli, M.; Ortar, G.; De Petrocellis, L. Arylboronic acids as dual-action FAAH and TRPV1 ligands. *Bioorg. Med. Chem. Lett.* **2016**, *26*, 1401–1405.

[55] Robertson, J. F. R. Fulvestrant (Faslodex®) – how to make a good drug better. *Oncologist* **2007**, *12*, 774–784.

[56] Chouinard, S.; Tessier, M.; Vernouillet, G.; Gauthier, S.; Labrie, F.; Barbier, O.; Belanger, A. Inactivation of the pure antiestrogen fulvestrant and other synthetic estrogen molecules by UDP-glucuronosyltransferase 1A enzymes expressed in breast tissue. *Mol. Pharmacol.* **2006**, *69*, 908–920.

[57] Liu, J.; Zheng, S.; Akerstrom, V. L.; Yuan, C.; Ma, Y.; Zhong, Q.; Zhang, C.; Zhang, Q.; Guo, S.; Ma, P.; et al. Fulvestrant-3 Boronic Acid (ZB716): An orally bioavailable selective estrogen receptor downregulator (SERD). *J. Med. Chem.* **2016**, *59*, 8134–8140.

[58] Zhong, Q.; Zhang, C.; Zhang, Q.; Miele, L.; Zheng, S.; Wang, G. Boronic prodrug of 4-hydroxytamoxifen is more efficacious than tamoxifen with enhanced bioavailability independent of CYP2D6 status. *BMC Cancer* **2015**, *15*, 625.

[59] Canturk, Z.; Tunali, Y.; Korkmaz, S.; Gulbaş, Z. Cytotoxic and apoptotic effects of boron compounds on leukemia cell line. *Cytotechnology* **2016**, *68*, 87–93.

[60] Liu, S.; Chang, C. N.; Verma, M. S.; Hileeto, D.; Muntz, A.; Stahl, U.; Woods, J.; Jones, L. W.; Gu, F. X. Phenylboronic acid modified mucoadhesive nanoparticle drug carriers facilitate weekly treatment of experimentallyinduced dry eye syndrome. *Nano Res.* **2015**, *8*, 621–635.

[61] Ebdrup, S.; Jacobsen, P.; Farrington, A. D.; Vedso, P. Structure-activity relationship for aryl and heteroaryl boronic acid inhibitors of hormone-sensitive lipase. *Bioorg. Med. Chem.* **2005**, *13*, 2305–2312.

[62] Fu, H.; Fang, H.; Sun, J.; Wang, H.; Liu, A.; Sun, J.; Wu, Z. Boronic acid-based enzyme inhibitors: a review of recent progress. *Curr. Med. Chem.* **2014**, *21*, 3271–3280.

[63] Ogiyama, T.; Yamaguchi, M.; Kurikawa, N.; Honzumi, S.; Yamamoto, Y.; Sugiyama, D.; Inoue, S. Identification of a novel boronic acid as a potent, selective, and orally active hormone

sensitive lipase inhibitor. *Bioorg. Med. Chem.* **2016**, *24*, 3801–2807.

[64] Field-Smith, A.; Morgan, G. J.; Davies, F. E. Bortezomib (Velcade™) in the treatment of multiple myeloma. *Ther. Clin. Risk. Manag.* **2006**, *2*, 271–279.

[65] Chen, D.; Frezza, M.; Schmitt, S.; Kanwar, J.; Dou, Q. P. Bortezomib as the first proteasome inhibitor anticancer drug: Current status and future perspectives. *Curr. Cancer Drug Targets* **2011**, *11*, 239–253.

[66] Yu, L.; Bulychev, A.; O'Brien, L.; Riorden, W.; Yu, S.; Paton, M.; Cardoza, K.; Bannerman, B.; Kupperman, E. Abstract #2921: Pharmacokinetics and pharmacodynamics of a selective proteasome inhibitor MLN9708 in nonclinical species following either intravenous or oral administration. *Cancer Res.* **2009**, *69*, 2921.

[67] Kupperman, E.; Lee, E. C.; Cao, Y.; Bannerman, B.; Fitzgerald, M.; Berger, A.; Yu, J.; Yang, Y.; Hales, P.; Bruzzese, F.; et al. valuation of the proteasome inhibitor MLN9708 in preclinical models of human cancer. *Cancer Res.* **2010**, *70*, 1970–1980.

[68] Lee, E. C.; Fitzgerald, M.; Bannerman, B.; Donelan, J.; Bano, K.; Terkelsen, J.; Bradley, D. P.; Subakan, O.; Silva, M. D.; Liu, R.; et al. Antitumor activity of the investigational proteasome inhibitor MLN9708 in mouse models of B-cell and plasma cell malignancies. *Clin. Cancer Res.* **2011**, *17*, 7313–7323.

[69] Assouline, S. E.; Chang, J.; Cheson, B. D.; Rifkin, R.; Hamburg, S.; Reyes, R.; Hui, A. M.; Yu, J.; Gupta, N.; Di Bacco, A.; et al. Phase 1 dose-escalation study of IV ixazomib, an investigational proteasome inhibitor, in patients with relapsed/refractory lymphoma. *Blood Cancer J.* **2014**, *4*, e251.

[70] Raedler, L. A. Ninlaro (Ixazomib): First oral proteasome inhibitor approved for the treatment of patients with relapsed or refractory multiple myeloma. *Am. Health Drug Benefits* **2016**, *9*, 102–105.

[71] Milani, P.; Demasi, M.; de Rezende, L.; Amaral, A. T. d.; Andrade, L. H. Synthesis of l-cysteine-based boron compounds and their evaluation as proteasome inhibitors. *New J. Chem.* **2014**, *38*, 4859–4871.

[72] Momose, I.; Umezawa, Y.; Hirosawa, S.; Iijima, M.; Iinuma, H.; Ikeda, D. Synthesis and activity of tyropeptin A derivatives as potent and selective inhibitors of mammalian 20S proteasome. *Biosci. Biotechnol. Biochem* **2005**, *69*, 1733–1742.

[73] Watanabe, T.; Abe, H.; Momose, I.; Takahashi, Y.; Ikeda, D.; Akamatsu, Y. Structure-activity relationship of boronic acid derivatives of tyropeptin: proteasome inhibitors. *Bioorg. Med. Chem. Lett.* **2010**, *20*, 5839–5842.

[74] Momose, I.; Abe, H.; Watanabe, T.; Ohba, S.-i.; Yamazaki, K.; Dan, S.; Yamori, T.; Masuda, T.; Nomoto, A. Antitumor effects of tyropeptin-boronic acid derivatives: new proteasome inhibitors. *Cancer Sci.* **2014**, *105*, 1609–1615.

[75] Shi, J.; Lei, M.; Wu, W.; Feng, H.; Wang, J.; Chen, S.; Zhu, Y.; Hu, S.; Liu, Z.; Jiang, C. Design, synthesis and docking studies of novel dipeptidyl boronic acid proteasome inhibitors constructed from αα- and αβ-amino acids. *Bioorg. Med. Chem. Lett.* **2016**, *26*, 1958–1962.

[76] Ge, Y.; Li, A.; Wu, J.; Feng, H.; Wang, L.; Liu, H.; Xu, Y.; Xu, Q.; Zhao, L.; Li, Y. Design, synthesis and biological evaluation of novel non-peptide boronic acid derivatives as proteasome inhibitors. *Eur. J. Med. Chem.* **2017**, *128*, 180–191.

[77] Islam, M. N.; Islam, M. S.; Hoque, M. A.; Kato, T.; Nishino, N.; Ito, A.; Yoshida, M. Bicyclic tetrapeptide histone deacetylase inhibitors with methoxymethyl ketone and boronic acid zinc-binding groups. *Bioorg. Chem.* **2014**, *57*, 121–126.

[78] Jiménez-Aligaga, K.; Bermejo-Bescós, P.; Martín-Aragón, S.; Csákÿ, A. G. Discovery of alkenylboronic acids as neuroprotective agents affecting multiple biological targets involved in Alzheimer's disease. *Bioorg. Med. Chem. Lett.* **2013**, *23*, 426–429.

[79] Jung, S.-J.; Lee, J. Y.; Kim, T. H.; Lee, D.-E.; Jeon, J.; Yang, S. D.; Hur, M. G.; Min, J.-J.; Park, Y. D. Discovery of boronic acid-based fluorescent probes targeting amyloid-beta plaques in Alzheimer's disease. *Bioorg. Med. Chem. Lett.* **2016**, *26*, 1784–1728.

[80] Hoang, T. T.; Smith, T. P.; Raines, R. T. A boronic acid conjugate of angiogenin that shows ROS-responsive neuroprotective Activity. *Angew. Chem. Inter. Ed.* **2017**, *56*, 2619–2622.

[81] Soloway, A. H.; Tjarks, W.; Barnum, B. A.; Rong, F.-G.; Barth, R. F.; Codogni, I. M.; Wilson, J. G. The chemistry of neutron capture therapy. *Chem. Rev.* **1998**, *98*, 1515–1562.

[82] Achilli, C.; Jadhav, S. A.; Guidetti, G. F.; Ciana, A.; Abbonante, V.; Malara, A.; Fagnoni, M.; Torti, M.; Balduini, A.; Balduini, C.; et al. Folic acid-conjugated 4-amino-phenylboronate, a boron-containing compound designed for boron neutron capture therapy, is an unexpected agonist for human neutrophils and platelets. *Chem. Biol. Drug Des.* **2014**, *83*, 532–540.

[83] Hattori, Y.; Ishimura, M.; Ohta, Y.; Takenaka, H.; Watanabe, T.; Tanaka, H.; Ono, K.; Kirihata, M. Detection of boronic acid derivatives in cells using a fluorescent sensor. *Org. Biomol. Chem.* **2015**, *13*, 6927–6930.

[84] Hattori, Y.; Ishimura, M.; Ohta, Y.; Takenaka, H.; Kirihata, M. Visualization of boronic acid containing pharmaceuticals in live tumor cells using a fluorescent boronic acid sensor. *ACS Sen.* **2016**, *1*, 1394–1397.